Gene 695 (2019) 1–11

Contents lists available at ScienceDirect

Gene

journal homepage: www.elsevier.com/locate/gene

Research paper

Molecular cloning and functional characterization of elongase (*elovl5*) and fatty acyl desaturase (*fads2*) in sciaenid, *Nibea diacanthus* (Lacepède, 1802)

Weiguang Zou[a,1], Zhideng Lin[a,1], Yisheng Huang[b], Samwel Mchele Limbu[c,d], Xiaobo Wen[a,*]

[a] Guangdong Provincial Key Laboratory of Marine Biology, Shantou University, Shantou 515063, PR China
[b] College of Food Engineering and Biotechnology, Hanshan Normal University, Chaozhou 521041, PR China
[c] Laboratory of Aquaculture and Environmental Health, School of Life Sciences, East China Normal University, Shanghai 200241, PR China
[d] Department of Aquatic Sciences and Fisheries Technology, University of Dar es Salaam, P. O. Box 35064, Dar es Salaam, Tanzania

ARTICLE INFO

Keywords:
Elovl5
Fads2
HUFA
Nibea diacanthus

ABSTRACT

In the present paper, we investigated the molecular cloning and functional characterization of elongase of very long chain fatty acid (*elovl*) and fatty acyl desaturase (*fads*) genes in a marine teleost, *Nibea diacanthus*. The elongase cDNA sequence encoded a polypeptide of 294 amino acids exhibiting Elovl5 activity, which effectively elongated both C18 (18:2n − 6, 18:3n − 3 and 18:3n − 6) and C20 (20:4n − 6 and 20:5n − 3) polyunsaturated fatty acids. The desaturase cDNA sequence specified a polypeptide of 445 amino acids indicating Δ6 desaturation activity, which coul converted C18:2n − 6 and C18:3n − 3 to C18:3n − 6 and C18:4n − 3, respectively. Tissue distribution analysis by quantitative real-time PCR revealed that the *elovl5* was primarily expressed in intestine and liver, while the *fads2* was mainly expressed in liver and brain. These results increase our knowledge of the ability of endogenous highly unsaturated fatty acids (HUFA) biosynthesis in marine carnivorous fish.

1. Introduction

Highly unsaturated fatty acids (HUFA) are usually defined as polyunsaturated fatty acids (PUFA) with 20–22 carbon chain length and ≥3 double bonds, widely known as docosahexaenoic acid (DHA, 22:6n − 3), eicosapentaenoic acid (EPA, 20:5n − 3) and arachidonic acid (ARA, 20:4n − 6). Evidence gathered mainly from epidemiological studies and intervention trials have demonstrated that these compounds provide a variety of human health benefits including preventing cancer (e.g., colorectal, breast and prostate) (Gerber, 2012), boosting neural development (Hooijmans et al., 2012), reducing the risk of heart diseases and alleviating hypertension (Davidson, 2013; Ruxton et al., 2010). Therefore, increasing research interests have been attracted to clarify the HUFA biosynthesis pathway and potential regulation mechanism, especially in marine fish, which could supply the unique and rich source of HUFA for human consumption.

The biosynthesis of HUFA in all vertebrates including fish involves a succession of desaturation and elongation reactions from PUFA precursors, α-linolenic acid (ALA, 18:3n − 3) and linoleic acid (LA, 18:2n − 6) (Cook and Mcmaster, 2002; Monroig et al., 2011a; Tocher, 2003). Specifically, the production of arachidonic acid (ARA, 20:4n − 6) from LA and EPA from ALA first requires Δ6 desaturation to 18:3n − 6/18:4n − 3 catalyzed by Δ6 fatty acyl desaturase (Δ6 Fad), followed elongation to 20:3n − 6/20:4n − 3 by fatty acyl elongases and a further Δ5 desaturation catalyzed by Δ5 Fad (Cook and Mcmaster, 2002). Alternatively, a pathway for the synthesis ARA and EPA is achieved by an elongation followed by Δ8 and Δ5 desaturation steps (Monroig et al., 2011a; Wang et al., 2014). The DHA synthesis from EPA involves a more complicated pathway that requires two further elongation steps, a second Δ6 desaturation and a peroxisomal β-oxidation process by the so-called “Sprecher” pathway (Sprecher, 2000). In addition, previous findings have demonstrated that some teleosts are able to biosynthesize DHA directly via a Δ4 desaturation from 22:5n − 3, such as *Siganus canaliculatus* (Li et al., 2010), *Solea senegalensis* (Morais et al., 2012), *Chirostoma estor* (Fonseca-Madrigal et al., 2014) and *Channa striata* (Kuah et al., 2015).

It has been shown that mammals have two types of genes encoding different desaturase, namely Fads2 (Δ6 desaturase) and Fads1 (Δ5 desaturase) (Guillou et al., 2010). By contrast, teleost fish seem to have lost *fads1* during evolution. Up to now, the only exception was found in

Abbreviations: HUFA, highly unsaturated fatty acids; PUFA, polyunsaturated fatty acids; *elovl5*, elongation of very long chain fatty acids 5; Δ6 *fad*, Δ6 fatty acyl desaturase; DHA, docosahexaenoic acid; EPA, eicosapentaenoic acid; LNA, α-linolenic acid; LA, linoleic acid; ARA, arachidonic acid

* Corresponding author at: Guangdong Provincial Key Laboratory of Marine Biology, Shantou University, 243 Daxue Road, Shantou, Guangdong 515063, China.
E-mail address: wenxbo@stu.edu.cn (X. Wen).

[1] These authors contributed equally to the study.

https://doi.org/10.1016/j.gene.2019.01.033
Received 20 October 2018; Received in revised form 16 January 2019; Accepted 23 January 2019
Available online 10 February 2019
0378-1119/ © 2019 Elsevier B.V. All rights reserved.

Table 1
Primers used in this study.

Primer	Sequence (5′—3′)	Aim
Oligo-	AAGCAGTGGTATCAACGCAGAGTACXXXXX	First-strand cDNA synthesis
UPM (short)	CTAATACGACTCACTATAGGGC	RACE-PCR
UPM (long)	CTAATACGACTCACTATAGGGCAAGCAGTGGTATCAACGCAGAGT	RACE-PCR
NUP	AAGCAGTGGTATCAACGCAGAGT	RACE-PCR
FadF	ATGCAGCAGTAATAGAGGAT	Partial cDNA cloning
FadR	GATTTGAAAGTTGAGGTGTC	Partial cDNA cloning
Elovl5F	TCGACAACTACCCACCAACC	Partial cDNA cloning
Elovl5R	GCAGCGTGCTCCAAAGAT	Partial cDNA cloning
Fad 3-1	GCACGACTTTGGCCACCTGTCTG	3′ RACE
Fad 3-2	CGACTGGTTCACCGGACACCTCA	3′ RACE
Elovl5 3-1	GAGCTTGTTACCGCTGTGTGGCAT	3′ RACE
Elovl5 3-2	GCACCAGAACGGCTCTCCTGTATCA	3′ RACE
Fad 5-1	TGAAGACGTTGGGCTTCGCATGA	5′ RACE
Fad 5-2	CCTGCGTCTGAGCAATCGCCAGT	5′ RACE
Elovl5 5-1	GCATGGCTGGGATTGCCGAGAGG	5′ RACE
Elovl5 5-2	CATGCCACACAGCGGTAACAAGC	5′ RACE
ORF FadF	CCCAAGCTTACCAGGCCAGAGACAGCA	Expression
ORF FadR	CCGGAATTCAACGTCACTCCTTTTGGGTT	Expression
ORF Elovl5F	CCCAAGCTTTGACAAATGGAGACCTTCAA	Expression
ORF Elovl5R	CCGGAATTCCACGGTTTCTCAAATGTCAA	Expression
Q-FadF	TCGCTTCCTGTGCTGCTAT	qRT-PCR
Q-FadR	CTTCTCGTGGTCGATGTCC	qRT-PCR
Q-Elovl5F	CTATGTGCGCAGTCGTTTGG	qRT-PCR
Q-Elovl5R	CGTTCTGGTGCTCCTTCTTT	qRT-PCR
M13F	CGCCAGGGTTTTCCCAGTCACGAC	PCR screening
M13R	AGCGGATAACAATTTCACACAGGA	PCR screening
18S-F	CCTGAGAAACGGCTACCACATCC	qRT-PCR
18S-R	AGCAACTTTAGTATACGCTATTGGAG	qRT-PCR

Restriction sites for *Hin*dIII and *Eco*RI are underlined in primer ORF FadF, ORF Elovl5F and ORF FadR, ORF Elovl5R sequences. X = undisclosed base in the proprietary SMARTer oligo sequence.

the *Anguilla japonica*, which possesses a Fads1 with Δ5 desaturase capacity (Lopes-Marques et al., 2018). Teleost Fads2 enzymes exhibit much more varied substrate specificities, including Δ4 (Li et al., 2010; Morais et al., 2012; Fonseca-Madrigal et al., 2014; Kuah et al., 2015), Δ5 (Hamid et al., 2016), dual Δ6 and Δ5 (Hastings et al., 2001; Tanomman et al., 2013; Fonseca-Madrigal et al., 2014; Kuah et al., 2016; Oboh et al., 2016; Ferraz et al., 2018) and Δ8 desaturase activities (Monroig et al., 2011a). In contrast to the desaturases, the substrate specificities of elongase of very long-chain fatty acids (Elovl) is also very complex. Among the seven members of the Elovl family described in vertebrates (Guillou et al., 2010), only Elovl5, Elovl4 and Elovl2 are identified as key enzymes involved in the elongation of PUFA (Monroig et al., 2011b). Previous research have shown that marine fish lack Elovl2, which is primarily active on C20 to C22 PUFA (Agaba et al., 2004; Morais et al., 2009; Gregory and James, 2014; Oboh et al., 2016), while the presence of Elovl4 may partly compensate for the above mentioned absence of Elovl2 in marine species (Carmona-Antoñanzas et al., 2011; Monroig et al., 2011b; Kabeya et al., 2015; Monroig et al., 2012a; Li et al., 2017a; Jin et al., 2017). To date, *elovl5* have been cloned and functionally characterized from numerous fish species (Agaba et al., 2004; Hastings et al., 2004; Morais et al., 2009; Monroig et al., 2012a; Monroig et al., 2013; Kabeya et al., 2015; Li et al., 2016a). Results from these studies demonstrated that fish Elovl5, similar to mammalian homologues (Jakobsson et al., 2006), showed high activity towards C18 (C18:4n − 3 and C18:3n − 6) and C20 (C20:4n − 6 and C20:5n − 3) PUFA, with remarkably lower elongase capacity towards C22 substrates (Castro et al., 2016).

The sciaenid *Nibea diacanthus* is an important marine carnivorous fish, which is widely distributed along the southern China, Malaysia, northern Australia and Japan (Li et al., 2017b). *N. diacanthus* has attracted increasing research interest on ovary, embryonic and larval development (Zhang et al., 2006; Shen et al., 2007), artificial spawning and farming (Chen et al., 2011; Shi et al., 2004) and nutritional requirements (Li et al., 2016b, 2017b) due to its rapid growth, large size, delicious taste and high market value. However, to the best of our knowledge, currently no information is available on the molecular basis of HUFA biosynthesis in *N. diacanthus*. Therefore, in the present study, we investigated the cloning, tissue distribution and functional characterization of *elovl5* and *fads2*, which are involved in HUFA biosynthesis. These results increase our knowledge on the ability of endogenous HUFA biosynthesis in marine carnivorous fish.

2. Materials and methods

2.1. Sample collection

Five juvenile *N. diacanthus* (average body weight ± SEM; 325.63 ± 6.28 g) were collected from a commercial farm in Nan'Ao (Shantou, China) and used for cloning and tissue-specific exapression of *elovl5* and *fads2* genes. The fish were anaesthetized by using eugenol solution at a concentration of 40 mg L^{-1}. Nine tissues including anterior intestine, liver, spleen, white muscle, stomach, brain, kidney, eye and heart from each fish were sampled and immediately collected in 1.5 ml RNase-free centrifuge tubes, frozen in liquid nitrogen and then stored at −80 °C refrigerator until further processing. This research was approved by the Committee on the Ethics of Animal Experiments of Shantou University.

2.2. Molecular cloning of elovl5 and fads2 cDNAs

Fresh livers (about 50 mg) from *N. diacanthus* were used to isolate total RNA using TRIzol® Reagent (Invitrogen, USA) following manufacturer's specifications. The quantity and quality of total RNA were detected by the Thermo Scientific NanoDrop 2000 spectrophotometer (Thermo Scientific Nanodrop, USA) at the absorbance of 260/280 nm and the values of all RNA samples ranged from 1.88 to 2.02, showing good quality. We further determined the integrity by using a 1% (*w/v*) agarose gel (results not shown). The first strand cDNA was synthesized from 4 μg total RNA using PrimeScript™ II 1st Strand cDNA Synthesis Kit (Takara, Dalian, China).

The primers for *elovl5* (Elovl5F and Elovl5R) and *fads2* (FadF and FadR) were designed based on the alignment of *elovl5* and *fads2* cDNA sequences from *Larimichthys crocea* (**NP_001290303**) and (**NM_001303363**), *Nibea mitsukurii* (**FJ952143**) and (**GQ996729**) and *Argyrosomus regius* (**KC261977**) and (**KC261978**), respectively. An additional sequence from *Rachycentron canadum* (**FJ440239**) was used for *elovl5* primer design. The primers above were used for amplifying the partial cDNA sequences of *N. diacanthus elovl5* and *fads2* by polymerase chain reaction (PCR). The PCR reactions for both *elovl5* and *fads2* included an initial denaturation of 95 °C for 3 min, followed by 35 cycles of 95 °C/30 s, 59 °C/30 s and 72 °C/1 min, and with a final extension step at 72 °C for 5 min (2 × Taq PCR Mastermix, Tiangen, Beijing, China). The PCR products were determined on 1% agarose gel and then purified with a PCR purification kit (Tiangen, Beijing, China). The purified PCR products were ligated with the pMD19-T vector (Takara, Dalian, China) and transformed into competent *Escherichia coli* cells. The positive recombinant clones were identified by PCR screening by using M13R and M13F primers (Table 1), and subsequently sequenced by a commercial company (BGI, Shenzhen, China). Based on the obtained partial cDNA sequences, specific primers were then designed to produce the full-length cDNAs of *elovl5* and *fads2* by 5′ (primers Elovl5 3-1/Elovl5 3-2 and Fad 3-1/Fad 3-2 for *elovl5* and *fads2*, respectively) and 3′ (primers Elovl5 5-1/Elovl5 5-2 and Fad 5-1/Fad 5-2 for *elovl5* and *fads2*, respectively) rapid amplification of cDNA ends (RACE) PCR (Clontech, USA). The sequences of all PCR primers used in this study are shown in Table 1.

2.3. Sequence and phylogenetic analyses

Homology searches were performed by using BLAST at the National Center for Biotechnology Information (NCBI; http://www.ncbi.nlm.nih.gov/). The predicted amino acid sequences were obtained with the ORF Finder (http://www.ncbi.nlm.nih.gov/gorf/orfig.cgi). The multiple alignments were created using the DNAMAN software for windows. Phylogenetic analysis based on the amino acid sequences were constructed by the neighbor-joining method by using the MEGA version 5.0 software. Confidence in the resulting phylogenetic tree branch topology was measured through bootstrapping through 1000 iterations.

2.4. Tissue distribution of N. diacanthus elovl5 and fads2 mRNA

The mRNA level of *N.diacanthus elovl5* and *fads2* in various tissues, including anterior intestine, liver, spleen, white muscle, stomach, brain, kidney, eye and heart were determined by quantitative real-time PCR (qRT-PCR). Total RNA extraction from each sample was carried out as described above. The single-strand cDNA was synthesized using PrimeScript® RT reagent Kit with gDNA Eraser (Takara, Dalian, China) with 1 μg of total RNA and subsequently stored at −20 °C. The qRT-PCR was performed using the SYBR® Premix Ex Taq™ II Kit (Takara, Dalian, China) in a Light Cycler (Roche Diagnostics, USA) Sequence Detection System. The total reaction volume was 20 μl containing 10 μl of SYBR® Premix Ex Taq™ II, 2 μl of the five-fold diluted cDNA, 0.8 μl (10 mM) each of forward and reverse primers, and 6.4 μl of sterile distilled H_2O. The PCR program was 95 °C for 30 s, followed by 40 cycles of 95 °C for 5 s and 58 °C for 20 s. At the end of each PCR, a dissociation curve analysis of amplification products was run to confirm only one PCR product was amplified and detected. Each sample (five biological replicates) was run in triplicate and reactions without templates were used as negative controls. For normalization purposes, the stability of potential references genes including β-actin and 18S rRNA was tested using BestKeeper (Pfaffl et al., 2004). The results confirmed that 18S rRNA was more stable and was subsequently used as a reference gene to normalize the expression levels of the candidate genes. Standard curves were generated using five different dilutions (five biological replicates) of the cDNA samples and the amplification efficiency was analyzed according to the following eq. $E = 10^{(-1/Slope)} - 1$. The amplification efficiencies for all genes were roughly equal and ranged from 91 to 101%. The relative expression level of *elovl5* and *fads2* mRNA was determined using the $2^{-\Delta\Delta Ct}$ method (Livak and Schmittgen, 2001).

2.5. Heterologous expression of putative elongase and desaturase in yeast

The functions of the *N. diacanthus* Elovl5 and Fads2 proteins were conducted by expressing the PCR fragment corresponding to the open reading frame (ORF) in *Saccharomyces cerevisiae*. Primers (Elovl5: ORF Elovl5F and ORF Elovl5R; Fads2: ORF FadF and ORF FadR) containing restriction enzyme sites *Hin*dIII and *Eco*RI were designed for amplification of the *elovl5* and *fads2* ORFs from liver cDNA using Pfu PCR MasterMix (Tiangen, Beijing, China). PCR program consisted of an initial denaturation step at 95 °C for 3 min, followed by 30 cycles of denaturation at 95 °C for 30 s, annealing at 55 °C for 30 s, extension at 72 °C for 1 min 30 s, followed by a final extension at 72 °C for 5 min. The DNA fragments were then digested with the corresponding restriction endonucleases (Takara, Dalian, China) and ligated into a similarly restricted pYES2 yeast expression vector (Invitrogen, USA) to produce the constructs pYES2-Elovl5 and pYES2-Fads2. The recombinant plasmids were used to transform *S. cerevisiae* (strain INVSc1, Invitrogen, USA) using the S.C. EasyComp™ Transformation kit (Invitrogen, USA). Selection of yeast containing the pYES2-Elovl5 and pYES2-Fads2 constructs was done on *S. cerevisiae* minimal medium minus uracil ($SCMM^{-uracil}$). Culture of the recombinant yeast was carried out in $SCMM^{-uracil}$ broth as described previously (Hastings et al., 2001) using galactose induction of gene expression. The following fatty acids were used as substrates for yeast transformed with pYES2-Elovl5: C18:2n−6, C18:3n−3, C18:3n−6, C20:4n−6, C20:5n−3, C22:4n−6 and C22:5n−3; pYES2-Fads2: C18:2n−6, C18:3n−3, C20:3n−6, C20:3n−3, C20:2n−6, C20:4n−3, C22:4n−6 and C22:5n−3. The PUFA substrates were added to the yeast cultures at final concentrations of 0.5(C18), 0.75 (C20) and 1.0 (C22) mM as PUFA substrates since the uptake efficiency has been shown to decrease with increasing chain length (Zheng et al., 2009). After 2 days, yeast cells were harvested and washed by using Hank's balanced salt solution containing 1% fatty acid-free albumin for further analysis. Yeast transformed with pYES2 containing no insert were cultured under the same conditions as a control treatment. All fatty acid substrates (all ≥98% pure) used for the functional characterization assays, were purchased from Cayman Chemical Company. Butylated hydroxyl toluene (BHT), fatty acid-free bovine serum albumin (BSA), galactose, 3-(hydroxymethyl) pyridine, nitrogen base, raffinose, tergitol NP-40 and uracil dropout medium were obtained from Sigma Chemical Co.

The analyses of fatty acid compositions of transgenic yeast were determined as described by Lin et al. (2018). In brief, total lipids were extracted from the yeast samples with chloroform/methanol (2:1, *v*/v) containing 0.01% BHT as antioxidant according to Folch et al. (1957). Fatty acid methyl esters were subsequently prepared, extracted, purified and detected by gas chromatography (GC2010-plus, Shimadzu, Japan) as described previously (Hastings et al., 2001; Monroig et al., 2013). Conversions from PUFA substrates were calculated as the proportion of exogenously added substrate fatty acid converted to elongated and desaturated fatty acid products as [individual product area / (all products areas + substrate area)] × 100 (Li et al., 2010).

2.6. Statistical analysis

The mRNA levels of *elovl5* and *fads2* in different tissues are presented as means ± SEM (standard error of the mean) and analyzed by one-way analysis of variance (ANOVA) following confirmation of normality and homogeneity of variance tests. Tukey's multiple comparison test was used to detect significant differences among the means ($P < 0.05$). Statistical analyses were performed using SPSS 20.0 (SPSS, Chicago, IL, USA).

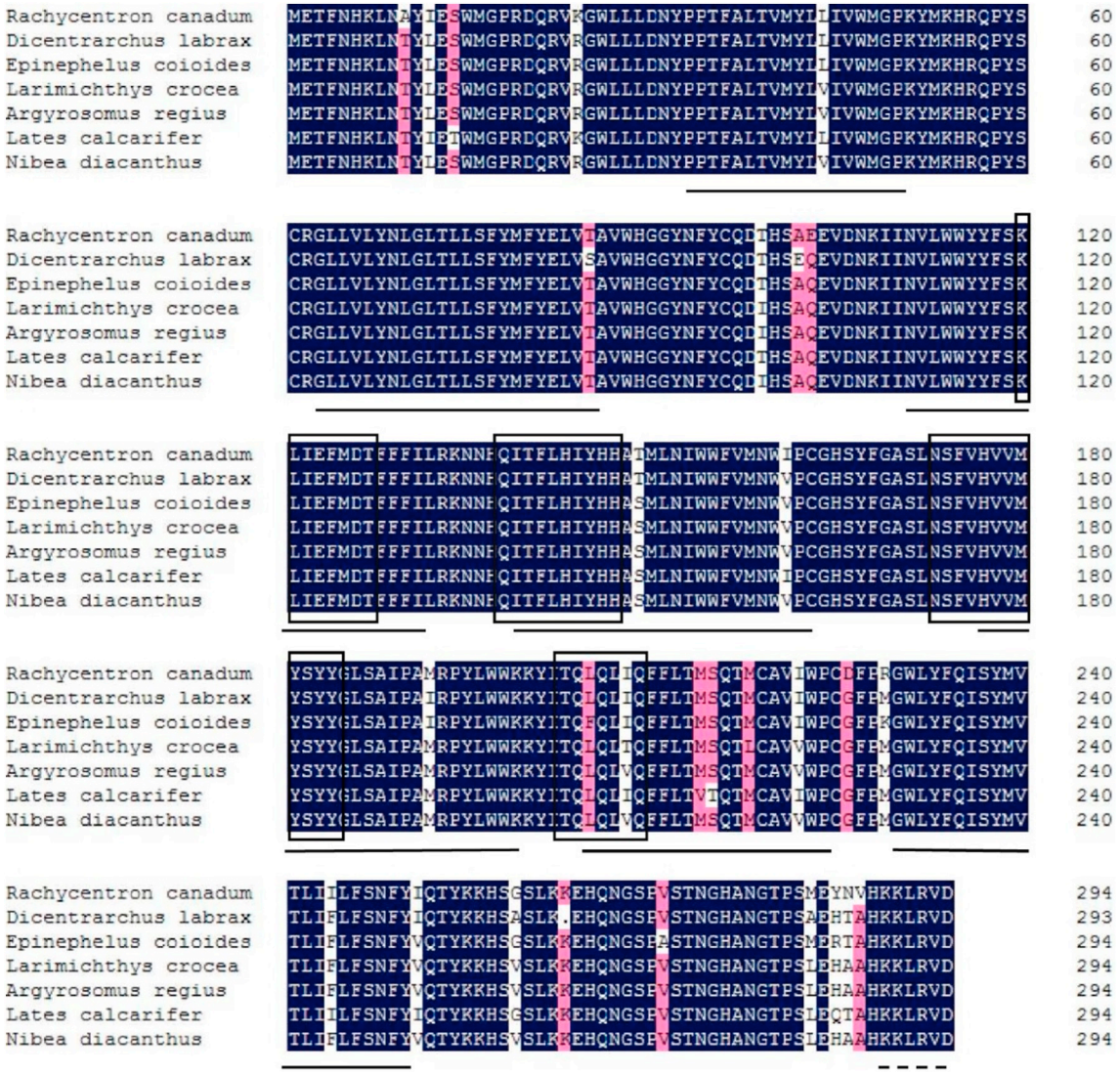


Fig. 1. A deduced amino acid sequence comparison of the *elovl5* from *Nibea diacanthus* with fatty acyl elongases from *Rachycentron canadum* (**ACJ65150**), *Dicentrarchus labrax* (**CBX53576**), *Epinephelus coioides* (**AGT80149**), *Larimichthys crocea* (**NP_001290303**), *Argyrosomus regius* (**AGG69479**), *Lates calcarifer* (**ACS91459**). The threshold for similarity shading was set at 75%. Identical residues are shaded black, and similar residues are shaded pink. Highly conserved motifs are boxed, the ER retention signal is dash-underlined and seven putative transmembrane domains are underlined. (For interpretation of the references to colour in this figure legend, the reader is referred to the web version of this article.)

3. Results

3.1. Sequence and phylogenetic analysis

The full-length sequence of *N. diacanthus elovl5* was 1273 bp containing a 5′ untranslated region (UTR) of 88 bp, a 3′-UTR of 300 bp with a polyA tail and an ORF of 885 bp encoding 294 amino acids. The sequence was submitted to GenBank database getting the accession number MF680836. The estimated molecular mass of deduced mature peptide was 35.07 kDa and the theoretical isoelectric point was 9.33. The results of multiple alignments showed that the protein sequence contained a single histidine box redox center motif (HXXHH), a putative endoplasmic reticulum (ER) retention signal at its carboxyl end, several highly conserved motifs (KXXEXXDT, QXXFLHXYHH, NXXXHXXMYXYY and TXXQXXQ) and multiple transmembrane-spanning domains (Fig. 1). In addition, *N. diacanthus* elongase indicated high identity with other Elovl5 amino acid sequences from various teleosts previously reported such as *A. regius* (100%), *N. mitsukurii* (99%), *R. canadum* (94%), *Epinephelus coioides* (86%) and L. *crocea* (83%) (Table 2). The phylogenetic analysis showed that *N. diacanthus elovl5* gene clustered together with their corresponding vertebrate orthologues and separated from other members of the *elovl* family clusters. In the branch of *elovl5*, all freshwater fish species and marine fish species

Table 2
Elovl5 sequences identities between *Nibea diacanthus* and 13 other organisms.

Matched species	Accession No.	% Identity
Argyrosomus regius	AGG69479	100
Nibea mitsukurii	ACR47973	99.3
Rachycentron canadum	ACJ65150	93.5
Epinephelus coioides	AGT80149	85.5
Larimichthys crocea	NP_001290303	83.4
Acanthopagrus schlegelii	ANJ04908	81.6
Dicentrarchus labrax	CBX53576	81.2
Lates calcarifer	ACS91459	80.0
Danio rerio	NP_956747	76.5
Mus musculus	NP_599016	71.2
Salmo salar	ACI62499	70.4
Homo sapiens	NP_068586	69.8
Pongo abelii	NP_001127147	68.9



Fig. 2. Phylogenetic relationship between the amino acid sequences of *elovl5* and 27 available elongases. The amino acid sequences were derived from the GenBank under the following accession numbers (in parentheses): *Homo sapiens*: Elovl1 (**NP_073732**), Elovl2 (**NP_060240**), Elovl3 (**NP_689523**), Elovl4 (**NP_073563**), Elovl5 (**NP_068586**), Elovl6 (**NP_076995**), Elovl7 (**NP_079206**); *Danio rerio*: Elovl5 (**NP_956747**), Elovl1 (**NP_001005989**); *Salmo salar*: Elovl5 (**NP_001005989**), Elovl4 (**NP_001182481**), Elovl2 (**ACI62500**); *Rachycentron canadum*: Elovl5 (**ACJ65150**), Elovl4 (**ADG59898**); *Larimichthys crocea*: Elovl5 (**NP_001290303**); *Argyrosomus regius*: Elovl5 (**AGG69479**); *Nibea mitsukurii*: Elovl5 (**ACR47973**); *Dicentrarchus labrax*: Elovl5 (**CBX53576**); *Lates calcarifer*: Elovl5 (**ACS91459**); *Epinephelus coioides*: Elovl5 (**AGT80149**); *Acanthopagrus schlegelii*: Elovl5 (**ANJ04908**); *Labru sbergylta*: Elovl5 (**XP_020510530**); *Xenopus tropicalis*: Elovl5 (**NP_001011248**); *Xenopus laevis*: Elovl5 (**NP_001089883**); *Bos taurus*: Elovl5 (**NP_001040062**); *Capra hircus*: Elovl5 (**BAF49682**); *Mus musculus*: Elovl5 (**NP_599016**). The tree was constructed using the neighbor joining method with MEGA 5.0. The horizontal branch length is proportional to amino acid substitution rate per site. Numbers represent the frequencies with which the tree topology presented was replicated after 1000 bootstrap iterations.

were clustered together and formed a sister group to the branch of other vertebrates, including orthologs from frog and some mammal species such mouse and human (Fig. 2).

The complete cDNA of *N. diacanthus fads2* was 1751 bp and contained an 1338 bp ORF, an 173 bp 5′ UTR and a 240 bp 3′-UTR with a poly (A) tail. The sequence was deposited in the GenBank database with the accession number MF737458. Sequence analysis revealed that the *fads2* cDNA encodes a polypeptide of 445 amino acids with predicted theoretical isoelectric point of 8.20 and molecular weight of 52.04 kDa. The protein sequence showed all the features of microsomal fatty acyl front-end desaturase, including three histidine-rich boxes, multiple transmembrane regions and an N-terminal cytochrome b_5 domain containing the heme-binding motif (H-P-G-G) (Fig. 3). The deduced polypeptide shares higher identity with Fads2 from teleosts including *Nibea coibor* (99%), *L. crocea* (99%) and *N. mitsukurii* (99%) (Table 3). The phylogenetic analysis revealed that *N. diacanthus fads2* gene grouped together with other teleost orthologs and clustered most closely to *fads2* from *A. regius*, *N. mitsukurii, N. coibor* and L. *crocea* (Fig. 4).

3.2. Tissue distributions of elovl5 and fads2 transcripts

The qRT-PCR was applied to determine mRNA expression level of *elovl5* and *fads2* in the tissues of healthy *N. diacanthus*, including anterior intestine, liver, spleen, white muscle, stomach, brain, kidney, eye and heart. The expression of *elovl5* was detected in all the examined tissues, although it showed obvious differences among tissues (Fig. 5). The expression of *elovl5* was strongly observed in anterior intestine and liver, and weakly in spleen, white muscle, stomach, brain, kidney, eye and heart (Fig. 7). In contrast, the *fads2* transcript was primarily expressed in the liver, with brain and eye showing the also high expression signals (Fig. 6).

3.3. Functional characterization in yeast

The functional characterizations of *N. diacanthus* Elovl5 and Fads2 proteins were investigated by determining the fatty acid profiles of transformed yeast with either empty pYES2 vector (control) or the vector containing *elovl5* ORF or *fads2* ORF inserts and grown in the

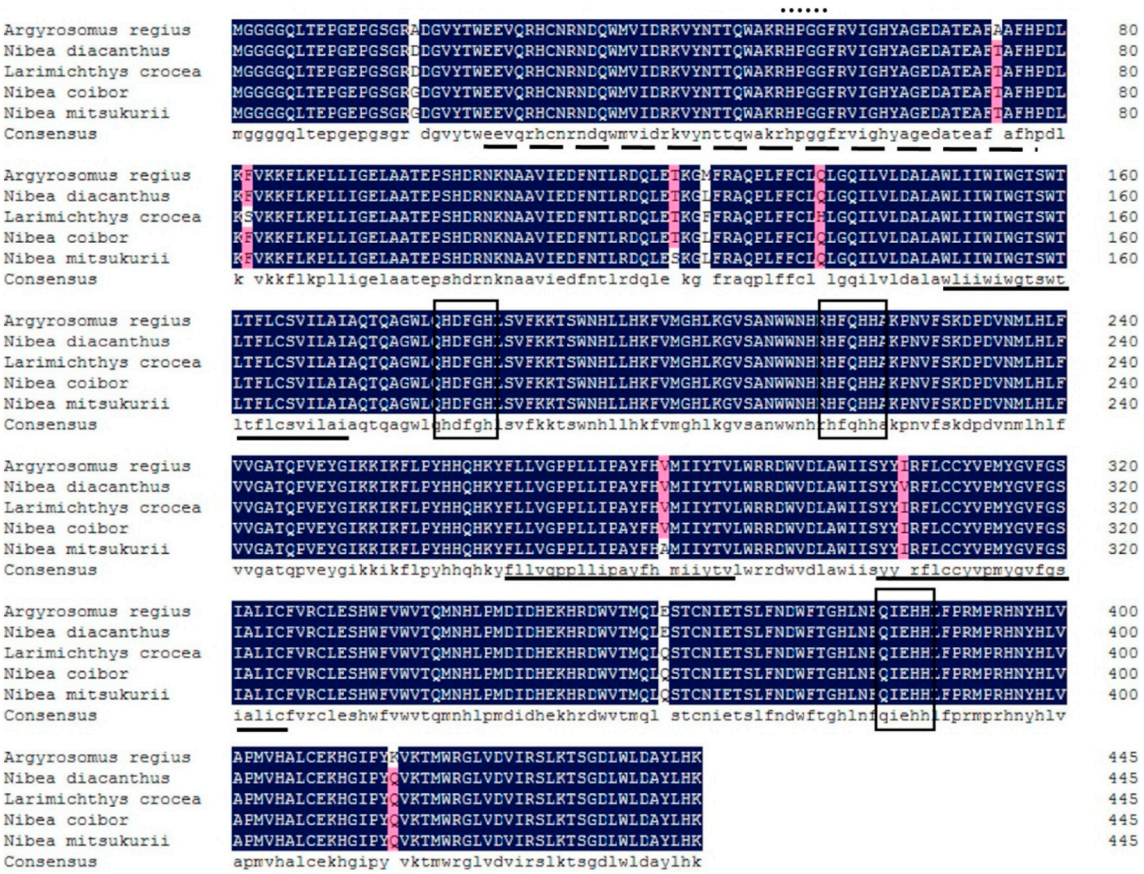


Fig. 3. A deduced amino acid sequence comparison of the *fads2* from *Nibea diacanthus* with fatty acyl desaturases from *Argyrosomus regius* (**AGG69480**), *Larimichthys crocea* (**NP_001290292**), *Nibea coibor* (**ASU87505**) and *Nibea mitsukurii* (**ACX54437**). The threshold for similarity shading was set at 75%. Identical residues are shaded black and similar residues are shaded pink. The dot-underlined at the top mark the heme-binding motif, HPGG. The cytochrome *b*5-like domain is dash underlined, the three putative transmembrane regions are underlined and the three histidine boxes (HXXXH, HXXXHH, HXXHH) are in the boxes. (For interpretation of the references to colour in this figure legend, the reader is referred to the web version of this article.)

Table 3
Fads2 sequences identities between *Nibea diacanthus* and 10 other organisms.

Matched species	Accession No.	% Identity
Nibea coibor	ASU87505	99
Larimichthys crocea	NP_001290292	99
Nibea mitsukurii	ACX54437	99
Argyrosomus regius	AGG69480	99
Sparus aurata	AAL17639	85
Acanthopagrus schlegelii	ANJ04910	85
Dicentrarchus labrax	ACD10793	84
Epinephelus coioides	ACJ26848	82
Siganus canaliculatus	ABR12315	74
Salmo salar	NP_001165752	73

presence of potential fatty acid substrates. The fatty acid composition of the wild yeast was characterized by having C16:0, C16:1n−7, C18:0 and C18:1n−9 as major components (Hastings et al., 2001). Thus yeast transformed with vector alone contained the four endogenous fatty acids above and whichever exogenous fatty acid was added. The detected results were consistent with *S. cerevisiae* lack of endogenous enzymatic capabilities for PUFA substrates as reported previously (Agaba et al., 2004; Li et al., 2010).

The fatty acid compositions of yeast transformed with pYES2-Elovl5 and pYES2-Fads2 constructs and grown in the presence of different substrates are shown in Figs. 7 and 8, respectively. The traces showed the major endogenous fatty acids (C16:0, C16:1n−7, C18:0 and C18:1n−9, peaks 1–4) and additional peaks corresponding to the substrates and elongation and desaturation products. Functional characterization of the *N. diacanthus* elongase revealed that the cloned cDNA encoded a protein with Elovl5 activity, which could effectively elongate both C18 substrates (18:3n−3, 18:2n−6 and 18:3n−6) and C20 substrates (20:5n−3 and 20:4n−6), whereas no elongation activity for C22 substrates (22:5n−3 and 22:4n−6) was detected (Table 4). The fatty acid profile of yeast transformed with pYES2-Fads2 showed extra peaks when grown in the presence of C18:3n−3 and C18:2n−6, which corresponded to C18:4n−3 and C18:3n−6, respectively. These data showed clearly that the cloned *N. diacanthus* desaturase had only Δ6 specificity, whereas Δ4, Δ5 and Δ8 activities were not detected (Table 5).

4. Discussion

Biosynthesis of the highly biologically active HUFA depends on the complement of desaturases and elongases, which convert the precursor ALA to EPA/DHA (Hastings et al., 2001). In the present study, we isolated and characterized the *elovl5* and *fads2* cDNAs from *N. diacanthus*. Both deduced amino acid sequences of *N. diacanthus elovl5* and *fads2* contained all the typical features of Elovl and Fad proteins, respectively. The amino acid sequence of *N. diacanthus* elongase possessed the highly conserved motifs of Elovl, such as KXXEXXDT, QXXFLHXYHH, NXXXHXXMYXYY and TXXQXXQ. Furthermore it showed high identity with Elovl5 from other teleosts, particularly *A. regius* (100%), *N. mitsukurii* (99%) and *R. canadum* (94%) (Zheng et al., 2009; Monroig et al., 2013; Yamamoto et al., 2010). The *N. diacanthus fads2* cDNA encoded a protein that had all the main structural features of desaturase including three histidine-rich boxes, a N-terminal

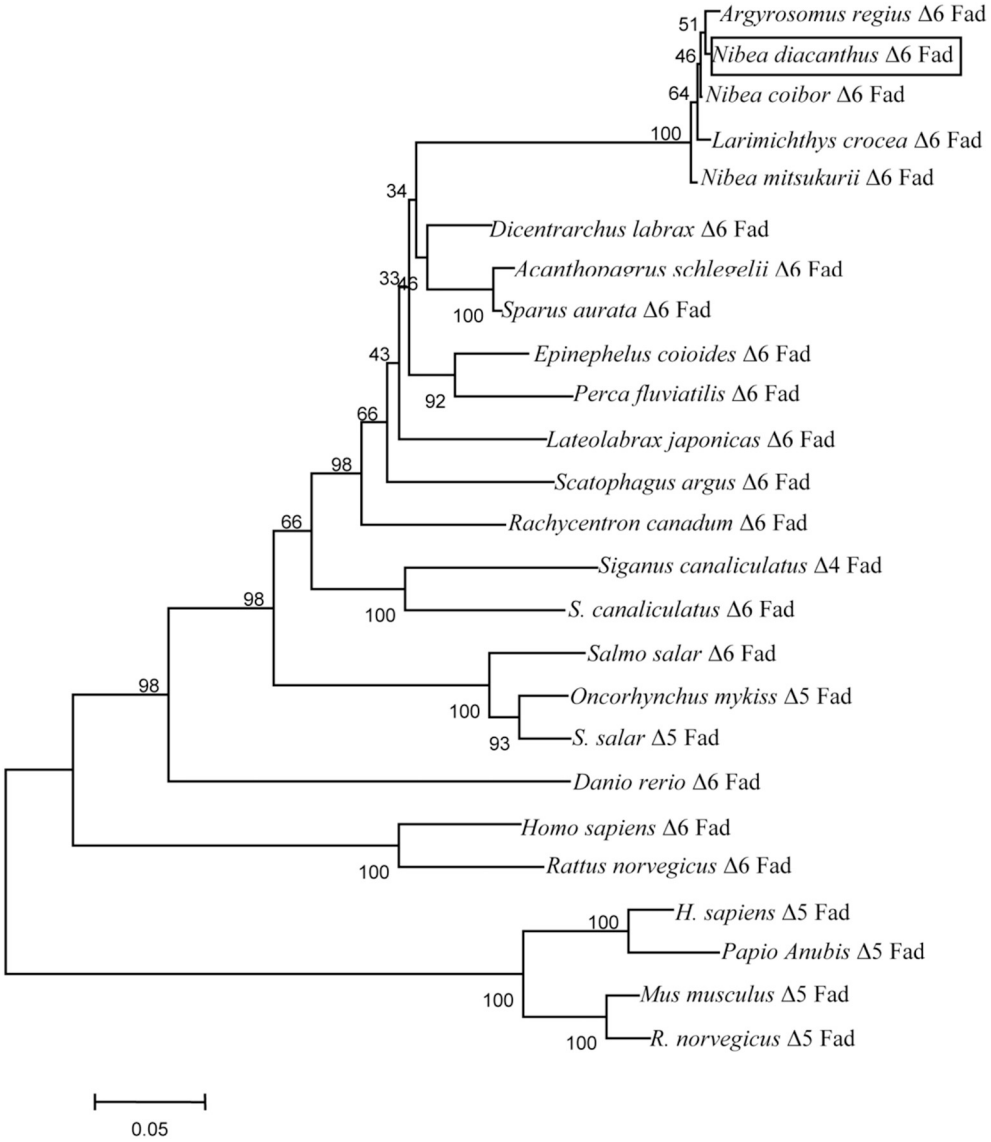


Fig. 4. Phylogenetic relationship between the amino acid sequences of *fads2* and 24 available desaturases. The amino acid sequences were derived from the GenBank under the following accession numbers (in parentheses): *Argyrosomus regius* (**AGG69480**); *Nibea coibor* (**ASU87505**); *Larimichthys crocea* (**NP_001290292**); *Nibea mitsukurii* (**ACX54437**); *Dicentrarchus labrax* (**ACD10793**); *Acanthopagrus schlegelii* (**ANJ04910**); *Sparus aurata* (**AAL17639**); *Epinephelus coioides* (**ACJ26848**); *Perca fluviatilis* (**AIY25022**); *Lateolabrax japonicas* (**AFZ87278**); *Scatophagus argus* (**AHA62794**); *Rachycentron canadum* (**ACJ65149**); *Siganus canaliculatus*: Δ6 Fad (**ABR12315**), Δ4 Fad (**ADJ29913**); *Salmo salar*: Δ6 Fad (**NP_001117047**), Δ5 Fad (**NP_001117014**); *Rattus norvegicus*: Δ6 Fad (**NP_112634**), Δ5 Fad (**NP_445897**); *Homo sapiens*: Δ6 Fad (**NP_004256**), Δ5 Fad (**AAF29378**); *Danio rerio* (**AAG25710**); *Mus musculus* (**NP_666206**); *Oncorhynchus mykiss* (**AFM77867**); *Papio anubis* (**ABP06289**). The tree was constructed using the neighbor joining method with MEGA 5.0. The horizontal branch length is proportional to amino acid substitution rate per site. Numbers represent the frequencies with which the tree topology presented was replicated after 1000 bootstrap iterations.

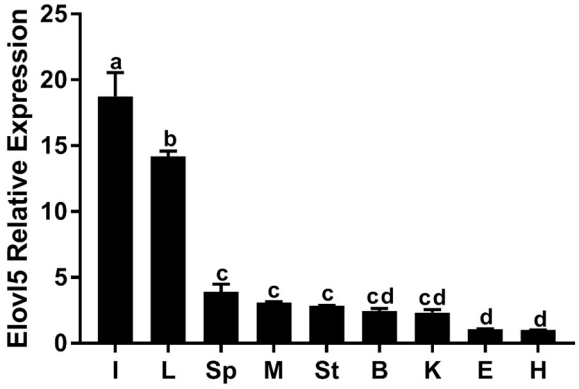


Fig. 5. Relative expression levels of *elovl5* mRNA in different tissues of *Nibea diacanthus*. Tissue expression was relative to that of heart. 18S was used as the reference gene for internal controls. Values are the mean ± SEM ($n = 5$) for each tissue. Different letters show significant differences ($P < 0.05$) among tissues as determined by one-way ANOVA followed by Tukey's multiple comparison test. I, intestine; L, liver; Sp, spleen; M, muscle; St, stomach; B, brain; K, kidney; E, eye; H, heart.

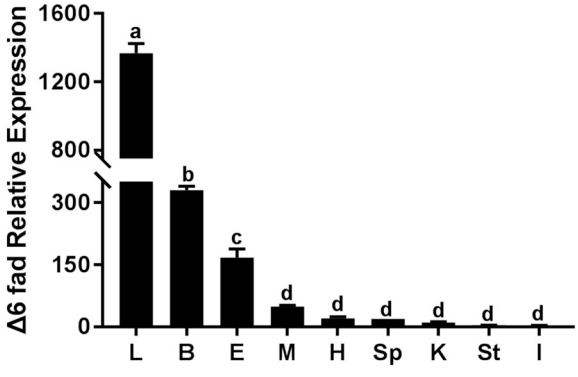


Fig. 6. Relative expression levels of *fads2* mRNA in different tissues of *Nibea diacanthus*. Tissue expression was relative to that of intestine. 18S was used as the reference gene for internal controls. Values are the mean ± SEM (n = 5) for each tissue. Different letters show significant differences ($P < 0.05$) among tissues as determined by one-way ANOVA followed by Tukey's multiple comparison test. I, intestine; L, liver; Sp, spleen; M, muscle; St, stomach; B, brain; K, kidney; E, eye; H, heart.

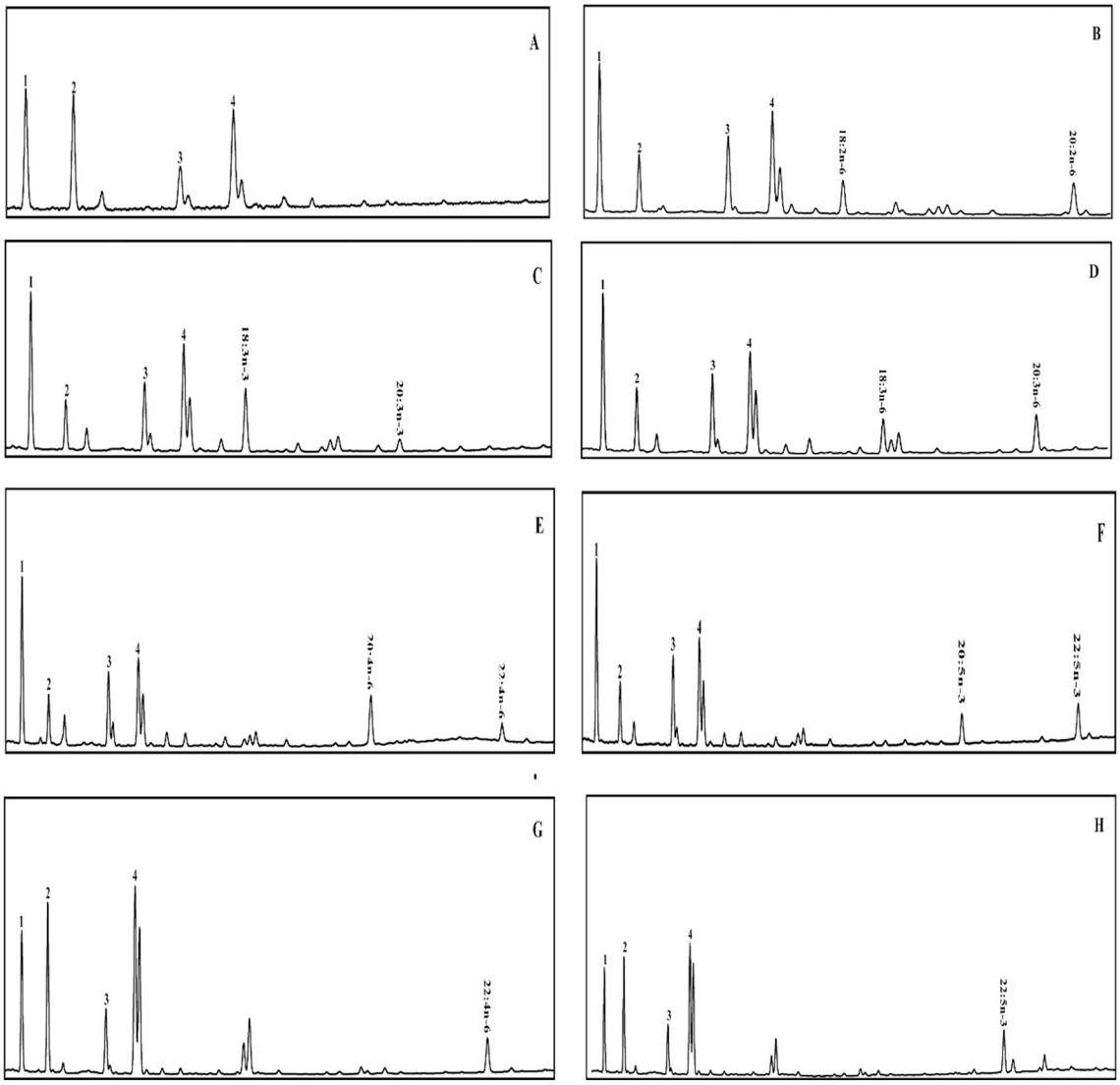


Fig. 7. Functional characterization of *Nibea diacanthus* putative Elovl5 in yeast *Saccharomyces cerevisiae*. Fatty acids were extracted from yeast transformed with the pYES2 vector alone or containing the ORF of the putative *elovl5* as an insert, growing in the presence of potential fatty acids substrates. A represent control group; B, C, D, E, F, G and H represent group that adds substrate of C18:2n − 6, C18:3n − 3, C18:3n − 6, C20:4n − 6, C20:5n − 3, C22:4n − 6 and C22:5n − 3. Peaks 1–4 represent four endogenous fatty acids of *S. cerevisiae*, including C16:0 (1), C16:1n − 7 (2), C18:0 (3) and C18:1n − 9 (4). Additionally, peaks derived from exogenously added substrates or elongated products are indicated accordingly.

cytochrome b_5 domain containing the heme-binding motif HPGG and three trans-membrane regions. The *N. diacanthus fads2* exhibited 73–99% similarity with Δ6 Fad from other teleosts (Geay et al., 2016; Xie et al., 2014; Zuo et al., 2016a). Phylogenetic analyses clearly showed each of the cloned genes to be orthologues of *elovl5* and *fads2* from other vertebrate species. Functional characterization by heterologous expression in *S. cerevisiae* confirmed that the functional activities of the Elovl5 having the ability to elongate C18 and C20 PUFA and the Fads2 possessing Δ6 desaturase activities. Collectively, results from conserved domains, similarity, phylogenetic analysis and functional characterization support that the elongase and desaturase genes identified in this study are *N. diacanthus elovl5* and *fads2*, respectively.

The tissue distributions of *elovl5* mRNA were primarily detected in liver and brain, which accords to previous studies among different teleosts, possibly indicating the importance of fatty acid metabolism and HUFA biosynthesis in these tissues.(Zheng et al., 2009; Monroig et al., 2012a; Monroig et al., 2013; Wang et al., 2014; Kuah et al., 2015; Li et al., 2016a; Zuo et al., 2016b). In this study, in addition to the high expression level in liver, the tissue distributions of *elovl5* transcript were also strongly observed in anterior intestine. Similar results were also observed in *Anguilla japonica* (Wang et al., 2014), *Salmo salar* (Morais et al., 2009) and *C. striata* (Kuah et al., 2015), which found the *elovl5* was highly expressed in intestine and liver. Besides, Lin et al. (2018) showed that the *N. coibor elovl5* mRNA was mainly detected in stomach. Intestine and stomach are now regarded as important sites of fatty acid metabolism (Bell et al., 2003; Lin et al., 2018). The high expression of *elovl5* in these tissues may participate in the process of converting the short chain fatty acids (16C and 18C) to the long chain fatty acids (18C, 20C and 22C) in intestinal tract (Bell et al., 2003; Zuo et al., 2016b; Lin et al., 2018). The *N. diacanthus fads2* had the highest expression level in the liver, with the brain and eye showing the next highest expression signals. This is consistent with the tissues expression pattern obtained from freshwater fish, such as *Cyprinus carpio* (Ren et al., 2012), *Oncorhynchus mykiss* (Seiliez et al., 2001) and *S. salar* (Zheng et al., 2005; Monroig et al., 2010). In contrast, other marine fish species showed the highest expression level of Δ6 *fad* mRNA in brain like *Gadus morhua* (Tocher et al., 2006), *R. canadum* (Zheng et al., 2009), *Lates calcarifer* (Mohd-Yusof et al., 2010), *Thunnus thynnus* (Betancor et al., 2017), *L .crocea* (Zuo et al., 2016a) and *N. coibor* (Lin et al., 2018). Both the *elovl5* and *fads2* from *N. diacanthus* showed high

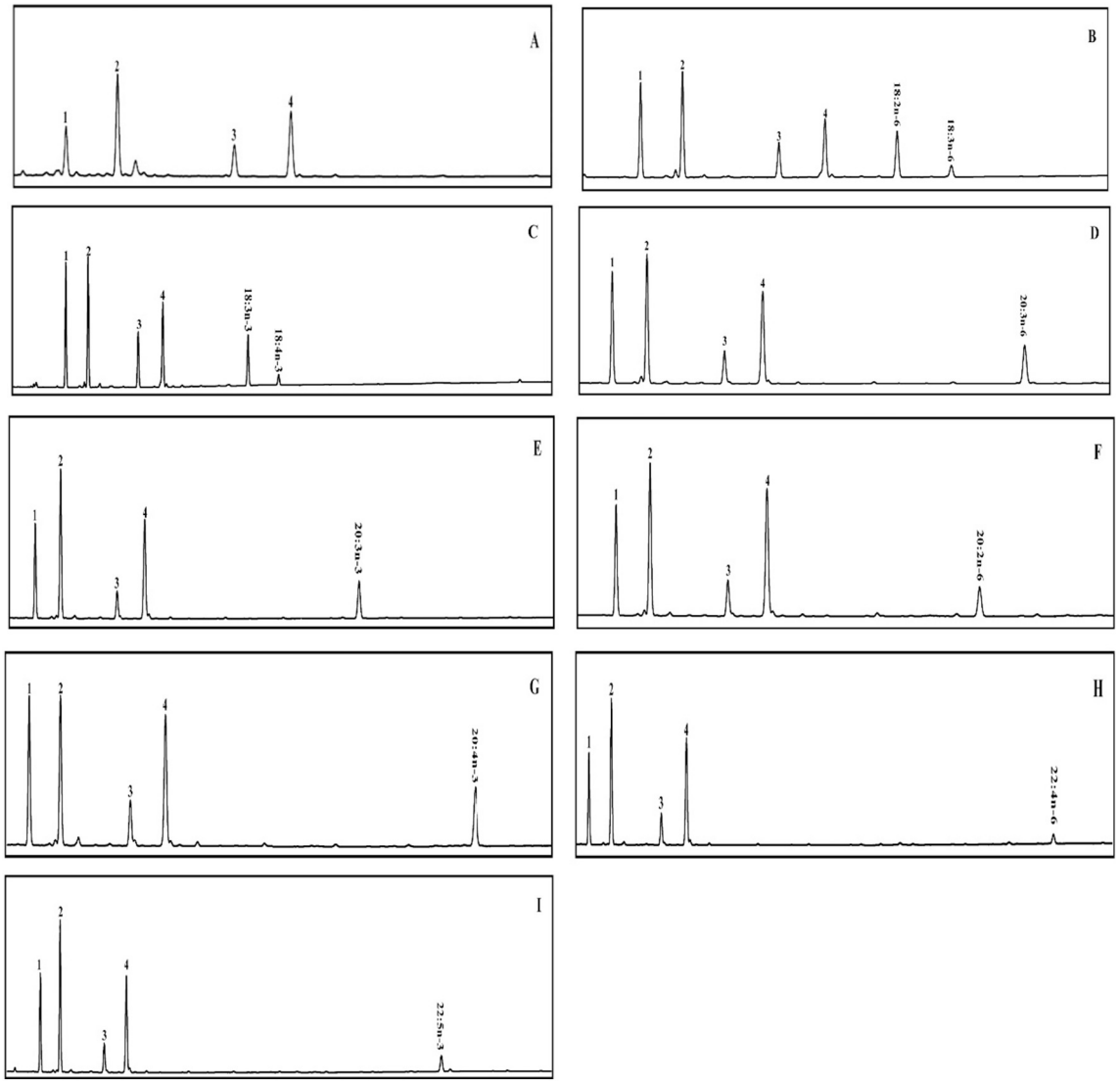


Fig. 8. Functional characterization of *Nibea diacanthus* putative Δ6 desaturase in transgenic *S. cerevisiae* transformed with pYES2 vector alone or containing desaturase cDNA ORF inserts, grown in the presence of potential fatty acid substrates. A represent control group; B, C, D, E, F, G, H and I represent group that adds substrate of C18:2n − 6, C18:3n − 3, C20:3n − 6, C20:3n − 3, C20:2n − 6, C20:4n − 3, C22:4n − 6 and C22:5n − 3. Peaks 1–4 represent four endogenous fatty acids of *S. cerevisiae*, including C16:0 (1), C16:1n − 7 (2), C18:0 (3) and C18:1n − 9 (4). Additionally, peaks derived from exogenously added substrates or desaturated products are indicated accordingly.

Table 4
Functional characterization of *Nibea diacanthus elovl5* in yeast *Saccharomyces cerevisiae*. Results are expressed as a percentage of total fatty acid substrate converted to elongated products.

Fatty acid substrate	Product	% Conversion	Activity
C18:2n − 6	C20:2n − 6	55.7	C18–20
C18:3n − 3	C20:3n − 3	17.3	C18–20
C18:3n − 6	C20:3n − 6	54.4	C18–20
C20:4n − 6	C22:4n − 6	21.5	C20–22
C20:5n − 3	C22:5n − 3	54.8	C20–22
C22:4n − 6	C24:4n − 6	Nd	C22–24
C22:5n − 3	C24:5n − 3	Nd	C22–24

Nd, not detected.

Table 5
Functional characterization of *Nibea diacanthus fads2* in yeast *Saccharomyces cerevisiae*. Results are expressed as a percentage of total fatty acid substrate converted to desaturated products.

Fatty acid substrate	Product	% Conversion	Activity
C18:2n − 6	C18:3n − 6	22.6	Δ6
C18:3n − 3	C18:4n − 3	19.2	Δ6
C20:3n − 6	C20:4n − 6	Nd	Δ5
C20:4n − 3	C20:5n − 3	Nd	Δ5
C20:3n − 3	C20:4n − 3	Nd	Δ8
C20:2n − 6	C20:3n − 6	Nd	Δ8
C22:5n − 3	C22:6n − 3	Nd	Δ4
C22:4n − 6	C22:5n − 6	Nd	Δ4

Nd, not detected.

expression in liver reflecting the importance of fatty acid metabolism and HUFA biosynthesis in this tissue.

In the present study, the functions of Elovl5 and Fads2 proteins from *N. diacanthus* were also determined by heterologous expression in yeast. The results showed that *N. diacanthus* Elovl5 had the capacity to elongate both C18 (C18:2n − 6, C18:3n − 3 and C18:3n − 6) and C20 (C20:4n − 6 and C20:5n − 3) PUFA substrates. However, *N. diacanthus* Elovl5 was unable to elongate C22 (C22:4n − 6 and C22:5n − 3) PUFA substrates. This result is similar to that in some teleosts such as

Acanthopagrus schlegelii (Kim et al., 2012), *A. japonica* (Wang et al., 2014), *E. coioides* (Li et al., 2016a) and *N. coibor* (Lin et al., 2018). On the other hand, the *N. diacanthus* Fads2 had the ability to convert 19.2% of C18:3n − 3 to C18:4n − 3 and 22.6% of C18:2n − 6 to C18:3n − 6, showing a Δ6 activity. Similarly, lower conversion efficiency for C18:3n − 3 and C18:2n − 6 were also observed in *N. mitsukurii* (Kabeya et al., 2015), *N. coibor* (Huang et al., 2017), *Dicentrarchus labrax* (González-Rovira et al., 2009) and *S. salar* (Monroig et al., 2010). However, in comparison with other marine fish species like *R. canadum* (Zheng et al., 2009), *A. japonica* (Wang et al., 2014), *S. canaliculatus* (Li et al., 2010) and *Scatophagus argus* (Xie et al., 2014), their Δ6 desaturases showed higher activity towards C18 PUFA and more active towards n − 3 PUFA substrates. Collectively, combining the functional characterizations of Elovl5 and Fads2, we demonstrated that *N. diacanthus* is capable of synthesizing C20:3n − 6 and C20:4n − 3 from 18:2n − 6 and 18:3n − 3, respectively.

In summary, the *elovl5* and *fads2* cDNA sequences from *N. diacanthus* liver were confirmed in the present study. Combining the results of tissue expression and functional characterization of the *elovl5* and *fads2* genes, we concluded that *N. diacanthus* had the ability to synthesize C20:3n − 6 and C20:4n − 3 from 18:2n − 6 and 18:3n − 3, respectively. Moreover, liver may play an important role in fatty acid metabolism and HUFA biosynthesis in *N. diacanthus*. These results increase our knowledge on the ability of endogenous HUFA biosynthesis in marine carnivorous fish.

Acknowledgments

The work was supported by Guangdong Oceanic and Fishery Science and Technology Foundation (No. A201005D06-1).

Declaration of interests

The authors declare no competing interests.

References

Agaba, M., Tocher, D.R., Dickson, C.A., Dick, J.R., Teale, A.J., 2004. Zebrafish cDNA encoding multifunctional fatty acid elongase involved in production of eicosapentaenoic (20:5n–3) and docosahexaenoic (22:6n–3) acids. Mar. Biotechnol. 6, 251–261.

Bell, M.V., Dick, J.R., Porter, A.E., 2003. Pyloric ceca are significant sites of newly synthesized 22:6n–3 in rainbow trout (*Oncorhynchus mykiss*). Lipids 38, 39–44.

Betancor, M.B., Ortega, A., De la Gándara, F., Tocher, D.R., Mourente, G., 2017. Lipid metabolism-related gene expression pattern of Atlantic bluefin tuna (*Thunnus thynnus* L.) larvae fed on live prey. Fish Physiol. Biochem. 43, 493.

Carmona-Antoñanzas, G., Monroig, O., Dick, J.R., Davie, A., Tocher, D.R., 2011. Biosynthesis of very long-chain fatty acids (C > 24) in Atlantic salmon: cloning, functional characterisation, and tissue distribution of an Elovl4 elongase. Comp. Biochem. Physiol. 159B, 122–129.

Castro, L.F., Tocher, D.R., Monroig, O., 2016. Long-chain polyunsaturated fatty acid biosynthesis in chordates: insights into the evolution of fads and Elovl gene repertoire. Prog. Lipid Res. 62, 25–40.

Chen, H.D., Zheng, J.H., Shen, Z.K., 2011. Technique for artificial breeding of spotted drum *Nibea diacanthus*. Fish. Sci. 8, 501–504.

Cook, H.W., Mcmaster, C.R., 2002. Chapter 7 Fatty Acid Desaturation and Chain Elongation in Eukaryotes. Elsevier B.V.

Davidson, M.H., 2013. Omega-3 fatty acids: new insights into the pharmacology and biology of docosahexaenoic acid, docosapentaenoic acid, and eicosapentaenoic acid. Curr. Opin. Lipidol. 24, 467–474.

Ferraz, R.B., Kabeya, N., Lopes-Marques, M., Machado, A.M., Ribeiro, R.A., Salaro, A.L., Ozório, R., Castro, L.F., Monroig, Ó., 2018. A complete enzymatic capacity for long-chain polyunsaturated fatty acid biosynthesis is present in the Amazonian teleost tambaqui. Comp. Biochem. Physiol. B (in press).

Folch, J.M.L., Lees, M.P., Stanley, G.H.A.S., 1957. A sample method for the isolation and purification of total lipids from animal tissue. J. Biol. Chem. 226, 497–509.

Fonseca-Madrigal, J., Navarro, J.C., Hontoria, F., Tocher, D.R., Martinez-Palacios, C.A., Monroig, O., 2014. Diversification of substrate specificities in teleostei Fads2: characterization of Δ4 and Δ6Δ5 desaturases of *Chirostoma estor*. J. Lipid Res. 55, 1408–1419.

Geay, F., Tinti, E., Mellery, J., Michaux, C., Larondelle, Y., Perpète, E., Kestemont, P., 2016. Cloning and functional characterization of Δ6 fatty acid desaturase (FADS2) in Eurasian perch (*Perca fluviatilis*). Comp. Biochem. Physiol. 191B, 112–125.

Gerber, M., 2012. Omega-3 fatty acids and cancers: a systematic update review of epidemiological studies. Br. J. Nutr. 107 (Suppl. 2), S228.

González-Rovira, A., Mourente, G., Zheng, X., Tocher, D.R., Pendon, C., 2009. Molecular and functional characterization and expression analysis of a Δ6 fatty acyl desaturase cDNA of European sea bass (*Dicentrarchus labrax* L.). Aquaculture 298, 90–100.

Gregory, M.K., James, M.J., 2014. Rainbow trout (*Oncorhynchus mykiss*) Elov15 and Elov12 differ in selectivity for elongation of omega-3 docosapentaenoic acid. Biochim. Biophys. Acta 1841, 1656–1660.

Guillou, H., Zadravec, D., Martin, P.G., Jacobsson, A., 2010. The key roles of elongases and desaturases in mammalian fatty acid metabolism: insights from transgenic mice. Prog. Lipid Res. 49, 186–199.

Hamid, N.K.A., Carmonaantoñanzas, G., Monroig, Ó., Tocher, D.R., Turchini, G.M., Donald, J.A., 2016. Isolation and functional characterisation of a fads2 in rainbow trout (*Oncorhynchus mykiss*) with Δ5 desaturase activity. PLoS One 11, e0150770.

Hastings, N., Agaba, M., Tocher, D.R., Leaver, M.J., Dick, J.R., Sargent, J.R., Teale, A.J., 2001. A vertebrate fatty acid desaturase withΔ5 andΔ6 activities. Proc. Natl. Acad. Sci. U. S. A. 98, 14304–14309.

Hastings, N., Agaba, M.K., Tocher, D.R., Zheng, X., Dickson, C.A., Dick, J.R., Teale, A.J., 2004. Molecular cloning and functional characterization of fatty acyl desaturase and elongase cDNAs involved in the production of eicosapentaenoic and docosahexaenoic acids from α-linolenic acid in Atlantic salmon (*Salmo salar*). Mar. Biotechnol. 6, 463–474.

Hooijmans, C.R., Pasker-de Jong, P.C., de Vries, R.B., Ritskes-Hoitinga, M., 2012. The effects of long-term omega-3 fatty acid supplementation on cognition and Alzheimer's pathology in animal models of Alzheimer's disease: a systematic review and meta-analysis. J. Alzheimers Dis. 28, 191–209.

Huang, Y., Lin, Z., Rong, H., Hao, M., Zou, W., Li, S., Wen, X., 2017. Cloning, tissue distribution, functional characterization and nutritional regulation of Δ6 fatty acyl desaturase in chu's croaker *Nibea coibor*. Aquaculture 479, 208–216.

Jakobsson, A., Westerberg, R., Jacobsson, A., 2006. Fatty acid elongases in mammals: their regulation and roles in metabolism. Prog. Lipid Res. 45, 237.

Jin, M., Monroig, Ó., Navarro, J.C., Tocher, D.R., Zhou, Q.C., 2017. Molecular and functional characterisation of two elovl4 elongases involved in the biosynthesis of very long-chain (> C24) polyunsaturated fatty acids in black seabream *Acanthopagrus schlegelii*. Comp. Biochem. Physiol. 212B, 41–50.

Kabeya, N., Yamamoto, Y., Cummins, S.F., Elizur, A., Yazawa, R., Takeuchi, Y., Haga, Y., Satoh, S., Yoshizaki, G., 2015. Polyunsaturated fatty acid metabolism in a marine teleost, Nibe croaker *Nibea mitsukurii*: functional characterization of Fads2 desaturase and Elovl5 and Elovl4 elongases. Comp. Biochem. Physiol. 188B, 37–45.

Kim, S.H., Kim, J.B., Jang, Y.S., Kim, S.Y., Roh, K.H., Kim, H.U., Lee, K.R., Park, J.S., 2012. Isolation and functional characterization of polyunsaturated fatty acid elongase (AsELOVL5) gene from black seabream (*Acanthopagrus schlegelii*). Biotechnol. Lett. 34, 261–268.

Kuah, M.K., Jayaram, A., Shuchien, A.C., 2015. The capacity for long-chain polyunsaturated fatty acid synthesis in a carnivorous vertebrate: functional characterisation and nutritional regulation of a Fads2 fatty acyl desaturase with Δ4 activity and an Elovl5 elongase in striped snakehead (*Channa striata*). Biochim. Biophys. Acta 1851, 248–260.

Kuah, M.K., Jaya-Ram, A., Shu-Chien, A.C., 2016. A fatty acyl desaturase (fads2) with dual Δ6 and Δ5 activities from the freshwater carnivorous striped snakehead *Channa striata*. Comp. Biochem. Physiol. 201A, 146–155.

Li, Y., Monroig, O., Zhang, L., Wang, S., Zheng, X., Dick, J.R., You, C., Tocher, D.R., 2010. Vertebrate fatty acyl desaturase with Δ4 activity. Proc. Natl. Acad. Sci. U. S. A. 107, 16840–16845.

Li, S., Yuan, Y., Wang, T., Xu, W., Li, M., Mai, K., Ai, Q., 2016a. Molecular cloning, functional characterization and nutritional regulation of the putative elongase Elovl5 in the orange-spotted grouper (*Epinephelus coioides*). PLoS One 11, e0150544.

Li, W., Wen, X., Zhao, J., Li, S., Zhu, D., 2016b. Effects of dietary protein levels on growth, feed utilization, body composition and ammonia-nitrogen excretion in juvenile *Nibea diacanthus*. Fish. Sci. 82, 137–146.

Li, S., Monroig, Ó., Navarro, J.C., Yuan, Y., Xu, W., Mai, K., Tocher, D.R., Ai, Q., 2017a. Molecular cloning and functional characterization of a putative Elovl4 gene and its expression in response to dietary fatty acid profiles in orange-spotted grouper Epinephelus coioides. Aquac. Res. 48, 537–552.

Li, W., Wen, X., Huang, Y., Zhao, J., Li, S., Zhu, D., 2017b. Effects of varying protein and lipid levels and protein-to-energy ratios on growth, feed utilization and body composition in juvenile *Nibea diacanthus*. Aquac. Nutr. 23, 1035–1047.

Lin, Z., Huang, Y., Zou, W., Rong, H., Hao, M., Wen, X., 2018. Cloning, tissue distribution, functional characterization and nutritional regulation of a fatty acyl Elovl5 elongase in chu's croaker *Nibea coibor*. Gene 659, 11–21.

Livak, K.J., Schmittgen, T.D., 2001. Analysis of relative gene expression data using real-time quantitative PCR and the $2^{(-\Delta\Delta C(T))}$ method. Methods 25, 402–408.

Lopes-Marques, M., Kabeya, N., Qian, Y., Ruivo, R., Santos, M., Venkatesh, B., Tocher, D.R., Castro, L.F., Monroig, Ó., 2018. Retention offatty acyl desaturase 1 (fads1) in Elopomorpha and Cyclostomata provides novel insights into the evolution of long-chain polyunsaturated fatty acid biosynthesis in vertebrates. BMC Evol. Biol. 18, 157.

Mohd-Yusof, N.Y., Monroig, O., Mohd-Adnan, A., Wan, K.L., Tocher, D.R., 2010. Investigation of highly unsaturated fatty acid metabolism in the Asian sea bass, *Lates calcarifer*. Fish Physiol. Biochem. 36, 827–843.

Monroig, Ó., Zheng, X., Morais, S., Leaver, M.J., Taggart, J.B., Tocher, D.R., 2010. Multiple genes for functional 6 fatty acyl desaturases (Fad) in Atlantic salmon *(Salmo salar* L.): gene and cDNA characterization, functional expression, tissue distribution and nutritional regulation. Biochim. Biophys. Acta 1801, 1072–1081.

Monroig, Ó., Li, Y., Tocher, D.R., 2011a. Delta-8 desaturation activity varies among fatty acyl desaturases of teleost fish: high activity in delta-6 desaturases of marine species. Comp. Biochem. Physiol. 159A, 206–213.

Monroig, Ó., Webb, K., Ibarra-Castro, L., Holt, G.J., Tocher, D.R., 2011b. Biosynthesis of

long-chain polyunsaturated fatty acids in marine fish: characterization of an Elovl4-like elongase from cobia *Rachycentron canadum* and activation of the pathway during early life stages. Aquaculture 312, 145–153.
Monroig, Ó., Wang, S., Zhang, L., You, C., Tocher, D.R., Li, Y., 2012a. Elongation of long-chain fatty acids in rabbitfish Siganus canaliculatus: cloning, functional characterisation and tissue distribution of Elovl5- and Elovl4-like elongases. Aquaculture 350-353, 63–70.
Monroig, Ó., Tocher, D.R., Hontoria, F., Navarro, J.C., 2013. Functional characterisation of a Fads2 fatty acyl desaturase with Δ6/Δ8 activity and an Elovl5 with C16, C18 and C20 elongase activity in the anadromous teleost meagre (*Argyrosomus regius*). Aquaculture 412, 14–22.
Morais, S., Monroig, Ó., Zheng, X., Leaver, M.J., Tocher, D.R., 2009. Highly unsaturated fatty acid synthesis in Atlantic salmon: characterization of ELOVL5- and ELOVL2-like Elongases. Mar. Biotechnol. 11, 627–639.
Morais, S., Castanheira, F., Martinez-Rubio, L., Conceição, L.E.C., Tocher, D.R., 2012. Long chain polyunsaturated fatty acid synthesis in a marine vertebrate: ontogenetic and nutritional regulation of a fatty acyl desaturase with Δ4 activity. Biochim. Biophys. Acta 1821, 660–671.
Oboh, A., Betancor, M.B., Tocher, D.R., Monroig, O., 2016. Biosynthesis of long-chain polyunsaturated fatty acids in the African catfish *Clarias gariepinus*: molecular cloning and functional characterisation of fatty acyl desaturase (fads2) and elongase (elovl2) cDNAs. Aquaculture 462, 70–79.
Pfaffl, M.W., Tichopad, A., Prgomet, C., Neuvians, T.P., 2004. Determination of stable housekeeping genes, differentially regulated target genes and sample integrity: BestKeeper-Excel-based tool using pair-wise correlations. Biotechnol. Lett. 26, 509–515.
Ren, H.T., Yu, J.H., Xu, P., Tang, Y.K., 2012. Influence of dietary fatty acids on muscle fatty acid composition and expression levels of Δ6 desaturase-like and Elovl5-like elongase in common carp (*Cyprinus carpio* var. Jian). Comp. Biochem. Physiol. 163B, 184–192.
Ruxton, C., Reed, S., Simpson, M., Millington, K., 2010. The health benefits of omega-3 polyunsaturated fatty acids: a review of the evidence. J. Hum. Nutr. Diet. 17, 449–459.
Seiliez, I., Panserat, S., Kaushik, S., Bergot, P., 2001. Cloning, tissue distribution and nutritional regulation of a Δ6 desaturase-like enzyme in rainbow trout. Comp. Biochem. Physiol. 163B, 83–93.
Shen, Z., Chen, H., Yao, R., Zhao, H., 2007. Seasonal cycles of ovary development of *Nibea diacanthus*. J. Guangdong Ocean Univ. 1, 7–11.
Shi, Z.H., Xia, L.J., Wang, J.G., 2004. A study on artificial propagation technique of *Nibea diacanthus*. Mar. Sci. 10, 34–37.
Sprecher, H., 2000. Metabolism of highly unsaturated n–3 and n–6 fatty acids. Biochim. Biophys. Acta 1486, 219–231.
Tanomman, S., Ketudat-Cairns, M., Jangprai, A., Boonanuntanasarn, S., 2013. Characterization of fatty acid delta-6 desaturase gene in Nile tilapia and heterogenous expression in *Saccharomyces cerevisiae*. Comp. Biochem. Physiol. 166B, 148–156.
Tocher, D.R., 2003. Metabolism and functions of lipids and fatty acids in teleost fish. Rev. Fish. Sci. 11, 107–184.
Tocher, D.R., Zheng, X., Schlechtriem, C., Hastings, N., Dick, J.R., Teale, A.J., 2006. Highly unsaturated fatty acid synthesis in marine fish: cloning, functional characterization, and nutritional regulation of fatty acyl Δ6 desaturase of Atlantic cod (*Gadus morhua* L.). Lipids 41, 1003–1016.
Wang, S., Monroig, Ó., Tang, G., Zhang, L., You, C., Tocher, D.R., Li, Y., 2014. Investigating long-chain polyunsaturated fatty acid biosynthesis in teleost fish: functional characterization of fatty acyl desaturase (Fads2) and Elovl5 elongase in the catadromous species, Japanese eel *Anguilla japonica*. Aquaculture 434, 57–65.
Xie, D., Chen, F., Lin, S., Wang, S., You, C., Monroig, Ó., Tocher, D.R., Li, Y., 2014. Cloning, functional characterization and nutritional regulation of Δ6 fatty acyl desaturase in the herbivorous euryhaline teleost *Scatophagus Argus*. PLoS One 9, e90200.
Yamamoto, Y., Kabeya, N., Takeuchi, Y., Alimuddin, Haga, Y., Satoh, S., Takeuchi, T., Yoshizaki, G., 2010. Cloning and nutritional regulation of polyunsaturated fatty acid desaturase and elongase of a marine teleost, the nibe croaker *Nibea mitsukurii*. Fish. Sci. 76, 463–472.
Zhang, Y.Z., Shi-Liu, H.U., Shen, X.U., Xie, Y.J., Jia-Cai, H.U., 2006. Study on early development of *Nibea diacanthus*. J. Jimei Univ. 1, 13–17.
Zheng, X., Tocher, D.R., Dickson, C.A., Bell, J.G., Teale, A.J., 2005. Highly unsaturated fatty acid synthesis in vertebrates: new insights with the cloning and characterization of a Δ6 desaturase of Atlantic salmon. Lipids 40, 13–24.
Zheng, X.Z., Ding, Z.K., Xu, Y.Q., Monroig, O., Morais, S., Tocher, D.R., 2009. Physiological roles of fatty acyl desaturases and elongases in marine fish: characterisation of cDNAs of fatty acyl Δ6 desaturase and elovl5 elongase of cobia (*Rachycentron canadum*). Aquaculture 290, 122–131.
Zuo, R., Mai, K., Xu, W., Dong, X., Ai, Q., 2016a. Molecular cloning, tissue distribution and nutritional regulation of a Δ6-fatty acyl desaturase-like enzyme in large yellow croaker (*Larimichthys crocea*). Aquac. Res. 47, 445–459.
Zuo, R., Mai, K., Xu, W., Dong, X., Ai, Q., 2016b. Molecular cloning, tissue distribution and nutritional regulation of a fatty acyl elovl5-like elongase in large yellow croaker, *Larimichthys crocea*. Aquac. Res. 47, 2393–2406.